



Get Clarity On Generics

Cost-Effective CT & MRI Contrast Agents

 **FRESENIUS
KABI**

[WATCH VIDEO](#)

AJNR

Tributary venosinus occlusion and septic cavernous sinus thrombosis: CT and MR findings.

B Schuknecht, D Simmen, C Yüksel and A Valavanis

AJNR Am J Neuroradiol 1998, 19 (4) 617-626

<http://www.ajnr.org/content/19/4/617>

This information is current as
of August 25, 2025.

Tributary Venosinus Occlusion and Septic Cavernous Sinus Thrombosis: CT and MR Findings

B. Schuknecht, D. Simmen, C. Yüksel, and A. Valavanis

PURPOSE: In autopsy reports of patients who died of septic cavernous sinus thrombosis, tributary venosinus occlusion has been a common finding related to intracranial inflammatory complications. The purpose of this article is to illustrate the MR and CT appearance of septic cavernous sinus thrombosis and tributary venous occlusion.

METHODS: Over a period of 7 years, eight patients with septic cavernous sinus thrombosis were examined by contrast-enhanced thin-section CT. The CT scans of these eight patients and those of 30 healthy control subjects were assessed independently and subjectively by two blinded readers to ascertain the presence, size, and density of areas of nonopacification within the cavernous sinus and the presence of filling defects and dilation of tributary veins and venous sinuses. In six subjects, MR images supplemented by a contrast-enhanced spoiled gradient-recalled acquisition in the steady state (SPGR) sequence were assessed with respect to the presence of filling defects, expansion, and signal abnormalities within the cavernous sinus and tributary veins and sinuses. The MR and CT findings were compared.

RESULTS: The CT studies of the eight patients were consistently differentiated from those of the control subjects by the two readers. Contrast-enhanced CT findings in patients included areas of nonopacification that were present within the cavernous sinus bilaterally in six cases and unilaterally in two. The size of the filling defects exceeded 7 mm in 76% of thrombosed cavernous sinuses compared with 9% of control subjects. The mean density of filling defects in patients differed significantly from those in control subjects. Comparison of the MR and CT findings in six cases showed the contrast-enhanced SPGR sequence to be equivalent to CT with respect to delineation of filling defects.

CONCLUSION: Contrast-enhanced high-resolution CT findings indicate that venosinus thrombosis associated with septic cavernous sinus thrombosis is not restricted to the superior ophthalmic vein and is more common than previously assumed. A contrast-enhanced SPGR MR sequence may be used as a reliable alternative to establish the diagnosis of cavernous sinus and tributary venosinus thrombosis.

Prior to the availability of CT and MR imaging, the diagnosis of cavernous sinus thrombosis was based solely on clinical criteria and, therefore, commonly reflected an advanced septic and thrombotic disease (1–4). In recent years, CT and MR imaging, by direct and indirect signs (5, 6), have contributed to an increased recognition of cavernous sinus thrombosis.

Considerable overlap between normal variations and pathologic abnormalities with respect to size and inner structure of the cavernous sinus, however, renders the interpretation of CT and MR studies difficult in early evaluations for the presence of septic cavernous sinus thrombosis.

As more patients survive as a result of improved therapy, morbidity, reported to range from 23% to 50% (7, 8), is gaining more attention. CT or MR examinations are required for early detection of intracranial complications of septic cavernous sinus thrombosis. Complications in the wake of cavernous sinus thrombosis may be due to arterial ischemia or venous obstruction. With high-resolution CT and MR imaging, cavernous carotid arterial wall inflammation has been increasingly recognized as a source of ischemic complications (9–11). However, little attention

Received September 15, 1997; accepted after revision November 24.

From the Institute of Neuroradiology (B.S., C.Y., A.V.) and the Department of ENT, Head and Neck Surgery (D.S.), University Hospital of Zurich.

Address reprint requests to B. Schuknecht, MD, Institute of Neuroradiology University Hospital of Zurich, CH 8091 Zurich, Switzerland.

TABLE 1: Summary of clinical and imaging findings in eight patients with cavernous sinus thrombosis

Case	Sex/ Age, y	Clinical Findings				Imaging Findings				
		Systemic Signs	Ophthalmic Signs	Cranial Nerve Deficit	Source of Infection	Cavernous Sinus Thrombosis	Ophthalmic Vein Thrombosis	Inferior Petrosal Sinus Thrombosis	Additional Sinus Thrombosis	Complications
1	F/42	Fever 38.6°C; Lc.* 13,400	Chemosis, eyelid edema, exophthalmos	R III	Sphenothmoidal	Bilateral	Bilateral	...	Sphenoparietal, bilateral	Abscess/hydrocephalus
2	F/20	Fever 39.8°C; Lc. 21,300	Eyelid edema	V ₁	Sphenoidal	Bilateral	...	Unilateral	Sphenoparietal, bilateral	Late abscess
3	F/67	Fever 39°C; Lc. 18,800	Chemosis, eyelid edema, exophthalmos	R III, VI; L VI	Facial	Bilateral	Unilateral	Bilateral
4	M/9	Fever 40°C; Lc. 10,800	...	R VI	Mastoidal	Bilateral	...	Unilateral	...	Carotid artery thrombosis
5	F/60	Fever; Lc. 10,800	Chemosis, eyelid edema	R VI	Ethmoidal	Bilateral	Unilateral	Carotid artery stenosis
6	M/4	Fever 40.5°C; Lc. 16,400	...	L VI, V ₁	Mastoidal	Bilateral	...	Unilateral	Sigmoid, unilateral	...
7	M/38	Fever 39°C; Lc. 14,500	...	R III	Sphenothmoidal	Unilateral	Carotid artery thrombosis
8	M/18	Fever 39°C; Lc. 14,500	Chemosis, eyelid edema, exophthalmos	L VI	Ethmoidal	Unilateral	Unilateral	Orbital abscess

* Lc signifies leucocyte count.

has been paid to the presence of concomitant venous sinus thrombosis in patients with septic cavernous sinus thrombosis apart from the common finding of thrombosis of the superior ophthalmic vein (5, 6). This is in contradiction to autopsy reports that have established the frequent involvement of the superior petrosal sinus (4), the inferior petrosal sinus (1, 12), and the sigmoid sinus (1, 12, 13) in patients with septic cavernous sinus thrombosis.

In this study, we analyzed the contrast-enhanced high-resolution CT findings in eight consecutive patients with the clinical diagnosis of septic cavernous sinus thrombosis in comparison with findings in 30 healthy control subjects. The CT examinations were also assessed with respect to the presence of concomitant venous sinus thrombosis. In six of the patients, MR examinations were performed to obtain the most sensitive imaging sequence for revealing the cavernous sinus as well as tributary venous sinus thrombosis.

Methods

Patients and Clinical Criteria

Eight patients (four males and four females; mean age, 32 years, range 4 to 67 years) with septic cavernous sinus thrombosis were examined with high-resolution CT and, in six cases, also with MR imaging. The clinical diagnosis of cavernous sinus thrombosis was based on a known site of septic infection in the vicinity of the cavernous sinus, ophthalmic signs indicative of venous congestion (eyelid edema, chemosis, protrusion bulbi), and a cranial nerve deficit (III, IV, V₁, or VI).

CT and MR Examinations

CT examinations were performed after intravenous bolus injection of 100 mL of nonionic contrast agent plus 100 mL of drip infusion. The axial examination consisted of 2-mm-thick contiguous sections with a 15° angulation inferior to the orbitomeatal plane. Direct coronal images were obtained in the prone position in six patients, while coronal reformations were obtained in two cases, in whom the clinical condition precluded direct coronal imaging.

The MR examinations in six patients (Table 1, cases 1, 2, 4, 5, 7, 8) consisted of a noncontrast coronal T1-weighted sequence (500/14–18 [TR/TE]) with 3-mm-thick sections. A T2-weighted axial series (2000–4500/80–108) with 4- to 4.5-mm-thick sections covered the entire brain. In every patient, an axial 3-D spoiled gradient-recalled acquisition in the steady state (SPGR) sequence was performed (25–52/2.5–7.9), with a flip angle of 20°, partition thickness of 0.7 to 1.0 mm, 18-cm field of view, and 256 × 128 matrix, before and after intravenous injection of contrast material (0.1 mmol/L per kg). Complementary coronal reformations or a coronal T1-weighted contrast-enhanced series were obtained.

Image Analysis

The axial CT scans of the eight patients were mixed with the axial CT scans of the 30 control subjects (60 cavernous sinuses) obtained according to the same protocol. First, the examinations were reanalyzed independently and subjectively in a blinded fashion by two neuroradiologists, who ascertained the presence (unilateral or bilateral) or absence of cavernous sinus thrombosis. Second, the cavernous sinuses of the eight patients were assessed by two authors with respect to the presence, size, and location of filling defects and the presence of sinus expansion, and were compared with findings in the control subjects. A filling defect was defined as a focal area of nonopacification

TABLE 2: CT findings in eight patients with cavernous sinus thrombosis compared with 30 control studies (axial plane)

	Cavernous Sinus			Tributary Veins/Sinuses	
	Patients (n = 16)	Control subjects (n = 60)		Patients (n = 16)	Control Subjects (n = 60)
Cavernous sinus			Superior ophthalmic vein		
Filling defects			Seen/not seen	16/0	60/0
None	2*	19	Filling defects	5	...
Single	10	25	Expansion	5	...
Multiple	4	16	Inferior petrosal sinus		
Size			Seen/not seen	9/7	37/23
<7 mm	3	40	Filling defects	5	...
≥7 mm	11	4	Expansion	5	...
Location			Sphenoparietal sinus		
Middle	11	23	Seen/not seen	13/3	31/29
Posterior	14	21	Filling defects	4	...
Size			Expansion	4	...
Ø†, mm	10.8 ± 1.2	8.3 ± 1.6			
Range, mm	9–12	6–13			
	n = 10	n = 20			
Filling defect Ø, HU	26.7 ± 7.8	–1.1 ± 12.3			
Density range	9–48	–40–36			

* Two patients with unilateral cavernous thrombosis.

† Ø signifies mean.

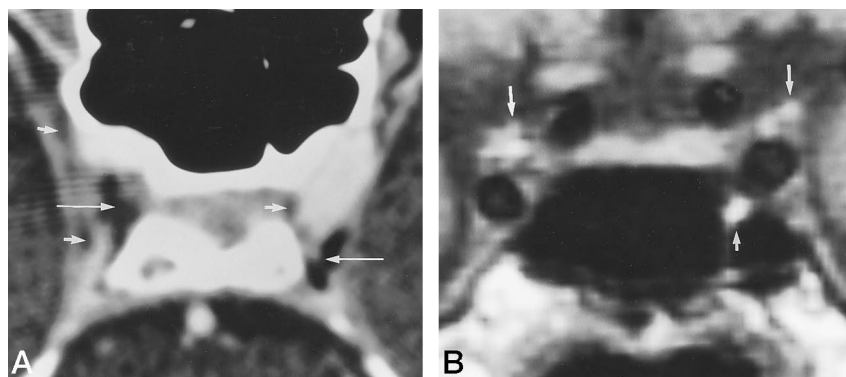


FIG 1. A, Axial contrast-enhanced CT scan in a healthy control subject shows an 8-mm filling defect of fat density within middle and posterior compartment of right cavernous sinus (*long arrows*) and smaller filling defect within left posterior cavernous sinus (*long arrows*). Additional small filling defects of fat density/signal intensity are present in the lateral right and medial left cavernous sinus (*short arrows*).

B, Coronal T1-weighted MR image (500/14) in same subject proves fat signal intensity of both structures (*long and short arrows*).

within the cavernous sinus that was not restricted to the lateral wall. Localization of these areas of nonopacification within the cavernous sinus was performed according to Hosoya et al (14). Filling defects in the anterior part were not included because of the proximity to fat in the orbital apex. In addition to the analysis of the cavernous sinus, the visibility and the presence of filling defects and expansion were assessed in the superior ophthalmic vein, the inferior petrosal sinus, and the sphenoparietal sinus.

Third, the size of the cavernous sinus was measured in patients as well as in the control subjects by one author. Measurements were performed on the hard copies of the axial examination lateral to the dorsum sellae to assure highest intraobserver reliability. Additional measurements were performed by the same author from the stored CT data from six patients (10 affected cavernous sinuses, cases 1, 2, 4, 5, 7, and 8) and 10 control subjects (20 cavernous sinuses). The CT data in two patients (cases 3 and 6) were unavailable for electronic analysis. The measurements included three density calculations obtained in the center of a single lesion or in the center of the largest lesion when multiple filling defects were present. The mean values and the range were compared between 10 affected cavernous sinuses and 20 control studies. These data and the measurements obtained from the hard copies (size of the cavernous sinus, size of filling defects) were analyzed statistically by using an unpaired *t*-test. In addition to the aforementioned investigations based on axial images, the axial and coronal CT scans of the eight patients were compared with respect to

visualization of filling defects and expansion within the cavernous sinus and tributary veins and venous sinuses (superior ophthalmic vein, inferior petrosal sinus, sphenoparietal sinus).

In six cases (Table 1, cases 1, 2, 4, 5, 7, and 8), the MR examinations were analyzed with respect to visualization of cavernous sinus thrombosis and tributary venous sinus thrombosis. The MR and CT findings were compared. The parameters assessed were the presence of areas of nonopacification on contrast-enhanced sequences, signs of venous sinus expansion, and the presence of signal intensity abnormalities on T1-weighted sequences. Owing to reported superiority of T1-weighted sequences (15, 16), heterogeneity of examination parameters on the T2-weighted sequences, and low spatial resolution, the latter sequence was not included in the analysis of signal intensity.

Results

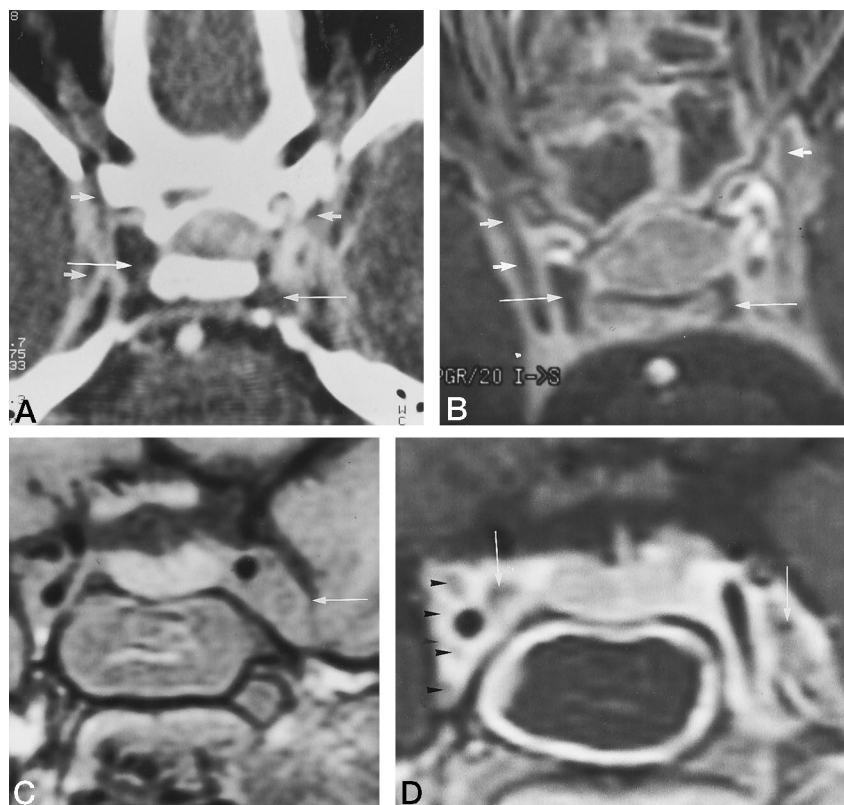
Cavernous Sinus Thrombosis

The patient data and clinical and imaging findings are summarized in Table 1. The blinded radiologists, using only axial CT scans, correctly identified all six patients with bilateral cavernous sinus thrombosis and the two patients with a unilateral cavernous sinus thrombosis. In one case (patient 8), however, unilat-

FIG 2. Extensive bilateral cavernous sinus thrombosis in a 20-year-old woman with a history of acute febrile sinusitis.

Contrast-enhanced axial CT scan (A) and SPGR MR image (22/3.4) with a 20° flip angle (B) reveal confluent large areas of nonopacification corresponding to thrombus formation in the middle and posterior compartments of the right cavernous sinus and in the posterior segment of the left cavernous sinus (*long arrows*). The smaller filling defects in the lateral compartments of the cavernous sinus (*short arrows*) show a tendency to coalesce on the MR image, which was obtained 2 days after the CT scan.

Noncontrast (C) and contrast-enhanced (D) coronal T1-weighted (500/14) MR images depict cavernous sinus expansion by cortex-isointense thrombus, particularly on the left (*arrowheads*). Filling defects differ in signal intensity from cranial nerves III, IV, V₁, VI, and V₂, indicated on the right (*arrow*).



eral cavernous sinus thrombosis was missed on the initial examination by both observers. The follow-up examination performed after 4 days was correctly interpreted as positive. Findings in all control subjects were considered normal by both blinded readers.

A large, confluent area of nonopacification that exceeded a size of 7 mm in the maximum dimension was present in 11 (79%) of 14 thrombosed cavernous sinuses (Table 2). In the control cases, however, only 9% of filling defects were larger than 7 mm (Fig 1). Single defects were more common among patients than among control subjects: 71% versus 61%. Seventy-five percent of filling defects in the control group were visually assessed as fat dense (Fig 1) and confirmed by density measurements. However, 25% of filling defects were of soft-tissue density (4 to 32 HU), and thus accounted for some overlap when compared with the density of thrombus in the patient group (mean, 27 HU; range, 9 to 48 HU). In addition to size and density, location of the area of nonopacification was a distinguishing factor. Whereas in patients with cavernous sinus thrombosis the posterior segment of the cavernous sinus was always involved (Fig 2), it was affected in only 21 (48%) of 44 cavernous sinuses in the control group.

Expansion of the cavernous sinus was assumed on the basis of size measurements of the 14 thrombosed cavernous sinuses: mean, 10.8 mm (SD, 1.2 mm) in patients as compared with 8.3 mm (SD, 1.6 mm) in the control group. The difference was statistically significant ($P < .001$). When contrast-enhanced CT scans in the axial and coronal plane were compared (Table 3), marked convexity of the lateral contour of

TABLE 3: Comparison of CT findings in eight patients with cavernous sinus thrombosis in the axial and coronal plane

CT Findings	Axial Plane	Coronal Plane
Cavernous sinus		
Filling defects	14/16	14/16
Lateral convexity	4/14*	12/14*
Superior ophthalmic vein		
Filling defects	5/16	5/16
Expansion	5/5*	5/5*
Inferior petrosal sinus		
Filling defects	5/9†	2/7†
Posterior convexity	5/5*	0/5*
Sphenoparietal sinus		
Filling defects	4/13†	4/10†
Expansion	4/4*	4/4*

* Number of thrombosed venous structures.

† Number of identified venous structures in a particular plane.

the cavernous sinus on coronal scans readily demonstrated expansion in 12 (86%) of 14 thrombosed sinuses. On axial scans, a straight or slightly lateral convexity of the dural border was visible in only four (29%) of 14 cases (Fig 2).

Additional Venosinus Occlusion

Criteria for recognizing tributary venosinus thrombosis associated with cavernous sinus thrombosis included the presence of filling defects and venous sinus expansion relative to findings in healthy control subjects. Unlike in the cavernous sinus, no filling defects were identified in any of the tributary venous sinuses

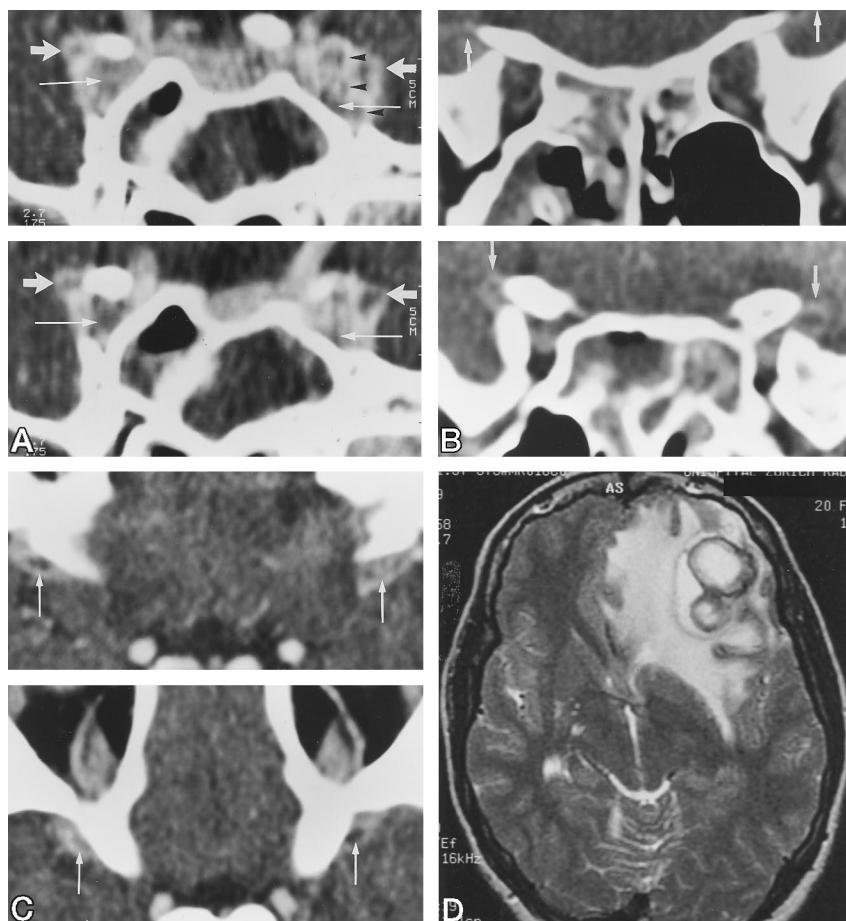


FIG 3. A, Coronal contrast-enhanced CT scan through middle and anterior cavernous sinus shows filling defects expanding cavernous sinus (long arrows) and sphenoparietal sinus (short arrows) bilaterally (arrowheads correspond to cranial nerves).

Sphenoparietal sinus thrombosis (arrows) is delineated on coronal (B) and axial (C) sections at the level of and above the anterior clinoid process. Note normal caliber of superior ophthalmic veins.

D, After 3 months, axial T2-weighted MR image (3500/98), obtained because of slight Broca's aphasia, reveals bilobular abscess in left inferior frontal gyrus and adjacent vasogenic edema.

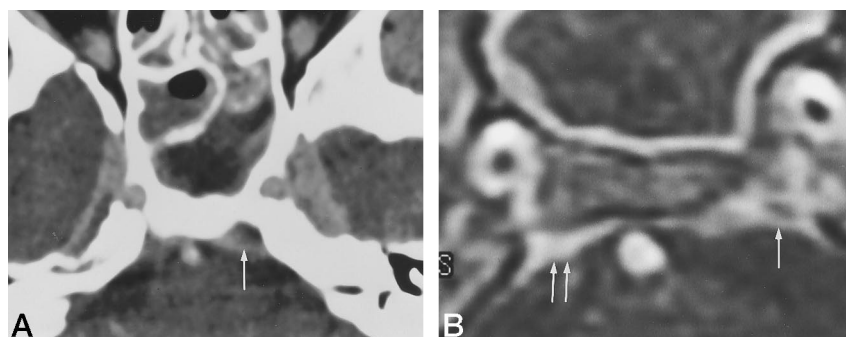


FIG 4. Axial contrast-enhanced CT scan (A) and corresponding contrast-enhanced SPGR MR image (B) depict left inferior petrosal sinus nonopacification and expansion (single arrow), indicating thrombosis. Note normal right inferior petrosal sinus (double arrows).

of the control subjects. Sphenoparietal sinus thrombosis appeared as a linear to oval filling defect with sinus dilatation relative to findings in control subjects. The sphenoparietal sinus was identified in 13 (81%) of 16 patients as compared with 31 (52%) of 60 control subjects (Table 2). Filling defects and expansion were seen bilaterally on consecutive axial and coronal CT scans in two patients. The thrombosed sinus could be traced from the anterior cavernous sinus along the sphenoid ridge toward the pterion (Fig 3). Cerebral abscess formation (Fig 3) occurred in both patients after 3 weeks and 3 months, respectively (Table 1, cases 1 and 2, respectively).

The inferior petrosal sinus is located in its own sulcus adjacent to the petrooccipital synchondrosis. It was seen as a cone-shaped structure in 37 (62%) of

the 60 control subjects and in nine (56%) of the 16 patients. A filling defect with significant sinus expansion was present in five of nine identified inferior petrosal sinuses, unilaterally in three patients and bilaterally in a single case. Thrombosis was best identified in the axial plane (Table 3) at the superior aspect of the inferior petrosal sinus as a triangular to oval area of nonopacification on both CT (Figs 4 and 5) and contrast-enhanced SPGR MR images (Fig 4). Unilateral thrombosis occurred on the more severely affected side of the cavernous sinus in three cases. Sigmoid sinus thrombosis associated with cavernous sinus thrombosis and inferior petrosal sinus thrombosis was encountered in a 4-year-old boy with acute mastoiditis (Fig 6).

Central nonopacification of the superior ophthalmic

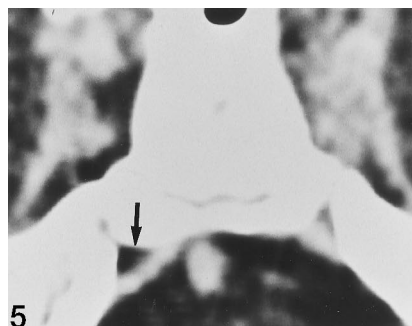


FIG 5. Axial contrast-enhanced CT scan in 9-year-old boy with bilateral cavernous sinus thrombosis due to acute right-sided mastoiditis. Confluent areas of thrombus formation are present within the cavernous sinus bilaterally, more pronounced on the right. Thrombosis is present in the right inferior petrosal sinus (straight arrow) while the left inferior petrosal sinus is spared.



FIG 6. Axial contrast-enhanced CT scan in 4-year-old boy with acute mastoiditis and subgaleal abscess on the left. Note multiple small partially confluent filling defects within the cavernous sinus bilaterally and left sigmoid sinus thrombosis (curved arrow). Note thrombus extension from left cavernous sinus to junction with inferior petrosal sinus (straight arrow).

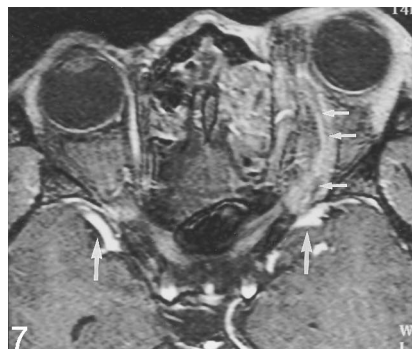


FIG 7. Contrast-enhanced SPGR MR image in 18-year-old man with progressive left-sided exophthalmos and chemosis shows linear filling defect in dilated left superior ophthalmic vein (short arrows). Note bilateral, predominantly left-sided ethmoidal inflammation and prominent but patent sphenoparietal sinus bilaterally (long arrows).

FIG 8. Right-sided exophthalmos in a 67-year-old woman 1 week after onset of bilateral cavernous sinus thrombosis due to right-sided facial phlegmon. Axial contrast-enhanced CT scan shows exophthalmos and extensive thrombus in dilated right superior ophthalmic vein.

mic vein was present in three of six patients with bilateral cavernous sinus thrombosis, bilaterally in one and unilaterally in two. In an additional one of two cases, unilateral superior ophthalmic vein thrombosis accompanied unilateral cavernous sinus thrombosis, accounting for five affected superior ophthalmic veins in four patients. The degree of superior ophthalmic vein expansion caused by the filling defect was found to vary considerably among patients (Figs 7 and 8).

Comparison of CT and MR Examinations

In six patients with 10 affected cavernous sinuses, CT findings were compared with MR findings (Table 4). The higher spatial resolution of SPGR images relative to noncontrast and contrast-enhanced T1-weighted images accounted for superior correlation with CT findings. This holds true with respect to delineation of filling defects within the cavernous sinus and tributary veins and sinuses. Filling defects were identified by contrast-enhanced CT and by SPGR MR sequences in 21 instances each, as compared with 16 instances on contrast-enhanced T1-weighted MR images.

Abnormal T1 signal intensity was noticed as gray matter isointense tissue in 10 of 10 cavernous sinuses and in seven of 11 tributary veins and sinuses. Expansion of the sphenoparietal and inferior petrosal sinus on T1-weighted images could not be assessed without contrast application, and in two instances was more apparent on CT scans than on SPGR images. The latter fact contributed to a slight superiority of CT

over the SPGR sequence. With a detection rate of 95% of the parameters, SPGR images were close to CT but surpassed T1-weighted noncontrast and contrast-enhanced MR sequences, which showed positive findings in 73% and 80% of criteria, respectively.

Discussion

Although cavernous sinus thrombosis has become rare, it remains a potentially life-threatening complication of an infection that may originate within the face, orbit, paranasal sinuses, or temporal bone (3, 17, 18). Therefore, all but one of our patients were primarily admitted to the department of ENT, where the diagnosis of septic cavernous sinus thrombosis was established. CT was the imaging technique of choice to confirm the suspected location of the underlying infectious process and to evaluate the osseous anatomy and integrity of the paranasal sinuses and temporal bone. As a consequence of CT-proved acute inflammation, all but one of our patients underwent either paranasal sinus surgery (five cases) or mastoidectomy (two cases). The confirmation of cavernous sinus thrombosis was of secondary importance after intraorbital or intracranial abscess formation had been ruled out.

A more benign course of septic cavernous sinus thrombosis has been observed in recent years (9, 10, 19). Earlier antibiotic treatment and a shift in pathogenesis have been assumed as causative factors. As with five of our patients, the origin of septic cavernous sinus thrombosis is increasingly recognized within

TABLE 4: Comparison of CT and MR findings in six patients with cavernous sinus thrombosis

	CT	MR Imaging			
		T2-Weighted	T1-Weighted	Contrast-Enhanced T1-Weighted	Contrast-Enhanced Spoiled Gradient-Recalled Acquisition in the steady state
Cavernous sinus					
Filling defect	10	8	10
Expansion	8	4	8	8	8
Signal intensity	...	Not analyzed	Iso 10
Superior ophthalmic vein					
Filling defects	4	2	4
Expansion	4	4	4	4	4
Signal intensity	...	Not analyzed	Iso 4
Inferior petrosal sinus					
Filling defects	3	2	3
Expansion	3	2	...	2	2
Signal intensity	...	Not analyzed	Iso 3
Sphenoparietal sinus					
Filling defects	4	4	4
Expansion	4	3	3
Signal intensity	...	Not analyzed
Positive parameters	40		29/40	32/40	38/40
	100%	...	72.5%	80%	95%

the sphenothmoidal sinus on CT and MR studies (5, 10, 11, 20–22).

Cross-sectional imaging techniques play an important role in the noninvasive assessment of patency or thrombosis of the dural venous sinuses. This also holds true for the cavernous sinus. However, unlike with other venous sinuses, contrast-enhanced CT has been favored as the primary imaging technique. This view is expressed in various case reports (19, 23–27) as well as in small series of four (6) and five (18, 28) patients. MR imaging, however, in contrast to radiologic studies of thrombosis of the convexity dural sinuses, has only rarely been used in the diagnostic workup for cavernous sinus thrombosis (10, 11, 20, 22, 29, 30). The largest series published consists of three patients (10), including one previously reported case (18). As with our patients, CT had been performed prior to MR imaging in all but one patient. The contribution of MR imaging to the diagnosis is, therefore, difficult to assess: in our study, it was of minor importance. A major objective was to assess the capability of different MR sequences in depicting the presence of thrombus within the cavernous sinus and tributary venous sinuses and to compare the findings with those obtained with contrast-enhanced CT.

The standards for a high-resolution CT examination of the cavernous sinus have been set by Kline et al (31, 32) and by Hasso et al (33). A section thickness of 1.5 mm and a table feed of 2 to 3 mm was recommended to depict normal anatomy and pathologic structures within the cavernous sinus. Our own protocol included 2-mm contrast-enhanced sections in the axial and coronal planes. For T1-weighted MR sequences, a section thickness of 3 mm has been considered appropriate (15, 34). This conforms to our protocol for the T1-weighted sequence. However, 3-D SPGR single-partition images of submillimeter

thickness provide higher anatomic resolution and better representation of the thrombosed compartments of the cavernous sinus as well as of adjacent veins after intravenous contrast application. Unlike CT, the contrast-enhanced MR examination was preceded by a noncontrast series to allow distinction between contrast enhancement and potentially high-signal methemoglobin.

Direct and indirect signs of septic cavernous sinus thrombosis have been reported, which, as in our patients, provide CT and MR evidence of a diagnosis that “is usually established on clinical grounds” (5). Direct signs include changes in density/signal intensity plus in the size and contour of the cavernous sinus (5, 6, 28, 31, 32). Areas of nonopacification in our patients had a tendency to coalesce; thus, on CT scans, they appeared as a single, large filling defect. In 11 (79%) of 14 cavernous sinuses, the maximum size equaled or exceeded 7 mm, whereas only 9% of filling defects in control subjects reached this size. These data conform to published CT data in 100 patients without Cushing disease in whom two (7%) of 27 intracavernous fat deposits exceeded 7 mm (35). The prevalence of fat is reported to be as low as 27% (35) and as high as 91% (14). In our control group, fat accounted for 75% of filling defects, whereas none of the patients with cavernous sinus thrombosis filling defects showed fat density.

In addition to fat, the presence of soft tissue within the cavernous sinus is well recognized (5, 15). The geometry of these structures was either longitudinal or round to oval on axial and coronal sections and thus frequently differed from the rather irregular areas of thrombosis. The intracavernous filling defects commonly extended medially and laterally to the carotid artery and therefore differed from soft-tissue-density neural structures confined to the lateral wall.

The latter correspond to cranial nerves III, IV, and V₁, and on axial images were always inseparable from the meningeal reflection of the lateral sinus wall. On coronal MR images (Fig 2D) and CT scans (Fig 3A) the cranial nerves were commonly identified. Connective tissue has been reported along the medial aspect of the cavernous sinus and along the course of the sixth nerve (15, 16). Together with the abducens nerve these may account for the soft-tissue-density filling defects seen in the control subjects.

Thrombus formation within the cavernous sinus venous spaces has been shown to cause replacement of variable signal intensity (15) by homogeneous, T1 cortex isointense tissue (10). This was confirmed in all six patients examined by MR imaging. T1 hyperintense signal was noticed in only one case within the lumen of the thrombosed cavernous carotid artery (9) but not within the thrombosed cavernous sinus venous spaces. The infectious process in cavernous sinus thrombosis appears to prolong methemoglobin formation and thus renders the diagnosis without convexity dural sinus thrombosis much more difficult on T1-weighted images. Owing to the larger section thickness and intersection gap, T2-weighted images provided insufficient resolution to be considered useful in the diagnosis of cavernous sinus thrombosis.

Expansion of the cavernous sinus due to the presence of thrombus was more reliably recognized on coronal as opposed to axial CT scans. In the axial plane, the lateral wall remained concave and thus appeared normal in 10 (71%) of 14 cavernous sinuses. On coronal images, marked lateral convexity was considered abnormal as compared with control subjects in 12 (86%) of 14 sinuses. Despite a significant difference in the transverse caliber between diseased cavernous sinuses in our patients and control subjects on axial images, the criterion itself appears to be of little value unless used in conjunction with other signs, such as filling defects or T1 signal intensity abnormalities.

Indirect signs are related to concomitant venous obstruction and consist of dilatation of the superior ophthalmic vein, exophthalmos, and increased dural enhancement along the lateral border of the cavernous sinus (5, 10, 28). Early thrombosis of the cavernous sinus evokes symptoms and signs of venous congestion, including eyelid edema, chemosis, and proptosis. These are the hallmarks of cavernous sinus thrombosis and were present in five of eight patients in our series.

The extracranial and intracranial venous connections with the cavernous sinus play an important role in the pathogenesis and symptomatology of cavernous sinus thrombosis and serve as pathways of potential complications. Septic cavernous sinus thrombosis begins as an infective thrombophlebitis (3, 17) that may reach the cavernous sinus by direct extension or venous embolism. Afferent connections to the cavernous sinus consist of the superior and inferior ophthalmic vein or penetrating veins from the posterior ethmoidal and sphenoidal sinuses. The circular (intercavernous) sinus and the sphenoparietal sinus are

also considered afferent. Efferent connections consist of the pterygoid plexus and emissary veins inferiorly and the superior and inferior petrosal sinus posteriorly. The veins and venous sinuses that communicate with the cavernous sinus are valveless, and therefore thrombophlebitis may affect the cavernous sinus in a retrograde fashion (3, 18).

At autopsy, secondary extension of the infectious thrombotic process has frequently been shown to involve other veins and venous sinuses (1, 4, 12, 13). Venosinus occlusion associated with septic cavernous sinus thrombosis has been reported as a common finding, with an assumed causal relationship to the fatal course of the patient (1, 12, 13). Thrombosis has not only been described in the superior ophthalmic vein (1, 4) but has been found to affect the superior petrosal sinus (4), the inferior petrosal sinus (1, 12), and the sigmoid sinus (1, 12, 13).

Superior ophthalmic vein thrombosis, even though one of the best known signs of cavernous sinus thrombosis, does not necessarily need to be present. It was identified in four (50%) of our patients as a linear filling defect with slight (Fig 7) to marked (Fig 8) expansion of the vein. In the largest series reported, superior ophthalmic vein thrombosis was described in three of four patients (6), in two of five patients (5), and in one of three patients (28). Superior ophthalmic vein thrombosis was not present in those two of our patients who had mastoiditis and in whom a retrograde route of infection to the cavernous sinus was likely (Table 1). On the other hand, the presence of chemosis and exophthalmos in our patients correlated with early involvement of the superior ophthalmic vein.

Inferior petrosal sinus thrombosis was shown by contrast-enhanced CT in four patients and by MR imaging in two patients, with five and three affected venous sinuses, respectively. In two patients with single inferior petrosal sinus thrombosis, MR imaging was not performed. In five inferior petrosal sinuses, the thrombus was identified on CT scans as a triangular filling defect in a markedly expanded sinus (Figs 4 and 5). On CT, a unilateral manifestation in three cases, expansion of the thrombosed sinus in all cases, and recanalization on follow-up studies in three of four cases allowed us to distinguish true thrombosis from beam-hardening artifacts along the petrooccipital synchondrosis. SPGR MR images were equivalent in demonstrating inferior petrosal sinus filling defects, even though expansion in one case was considered less pronounced relative to its appearance on CT scans (Fig 4). Inferior petrosal sinus thrombosis was present ipsilateral to acute mastoiditis in two patients, in one case in conjunction with sigmoid sinus thrombosis.

Sphenoparietal sinus thrombosis in two cases appeared as an oval to linear area of nonopacification on CT scans, SPGR MR sequences, and contrast-enhanced T1-weighted MR images, and could be traced along the sphenoid ridge from the anterolateral contour of the cavernous sinus to the pterion. Contrary to superior ophthalmic vein and inferior

petrosal sinus involvement, sphenoparietal sinus thrombosis was missed on noncontrast T1-weighted images, probably because of partial volume effects with CSF and adjacent hypointense bone. Sphenoparietal sinus thrombosis was present concomitant with bilateral superior ophthalmic vein thrombosis in one patient, in addition to unilateral inferior petrosal sinus thrombosis in the second case. In both patients with sphenoparietal sinus thrombosis, a cerebral abscess developed after 3 weeks and 3 months, respectively. The abscess occurred in the right temporal pole in the first case and in the inferior left frontal gyrus in the second case. Cerebral abscess formation following cavernous sinus thrombosis has been reviewed by Mahapatra et al (36). In the eight cases they reviewed, the frontal and temporal lobe were common locations for this complication, and the time interval varied from 3 to 6 months. The location in both instances and the time interval in one case were in conformity with findings in our patients. While the mode of spread is a matter for speculation, a hematogenous extension by way of a retrograde thrombophlebitis of the sphenoparietal sinus is likely (1, 3, 18, 36). Retrograde thrombophlebitis within the sphenoparietal sinus is promoted by venous congestion due to cavernous sinus thrombosis. Venous congestion with consecutive dilatation probably also accounts for the higher detection rate of the sphenoparietal sinus in our patients: 81% compared with 52% in the control subjects (Table 2). Tributary venosinus thrombosis, as found in two of our patients, may account for delayed or late cerebral complications. It is therefore less well recognized than concomitant arterial thrombosis, which may occur early in the wake of cavernous sinus thrombosis. The autopsy appearance of inflammatory internal carotid artery occlusion has been described only once (4), but it was reported in an additional 27 cases at angiography, CT, and MR imaging (9).

Conclusion

The prevalence of tributary venosinus thrombosis associated with septic cavernous sinus thrombosis is probably underestimated. The presence of a large filling defect of non-fat density or signal intensity with sinus expansion as an objective parameter is the most reliable criterion by which to establish the diagnosis of cavernous sinus thrombosis and to recognize tributary venosinus thrombosis on contrast-enhanced CT or MR studies. Thrombosis of the superior ophthalmic vein and the inferior petrosal and sigmoid sinuses was not associated with intracranial complications. However, delayed frontotemporal abscess formation occurred in both our patients with thrombosis of the sphenoparietal sinus.

Acknowledgment

We thank A. Gebauer for assessment of the examinations of patients and control subjects. B. Albers is acknowledged for providing help with the manuscript.

References

1. Dixon OJ. **The pathologic examination in cavernous sinus thrombosis.** *JAMA* 1926;87:1088-1092
2. Grove WE. **Septic and aseptic types of thrombosis of the cavernous sinus.** *Arch Otolaryngol* 1936;24:29-50
3. Shaw RE. **Cavernous sinus thrombophlebitis: a review.** *Br J Surg* 1952;40:40-48
4. Weisman AD. **Cavernous-sinus thrombophlebitis.** *N Engl J Med* 1944;231:118-122
5. De Slegte RGM, Kaiser MC, van der Baan S, Smit L. **Computed tomographic diagnosis of septic sinus thrombosis and their complications.** *Neuroradiology* 1988;30:160-165
6. Ahmadi J, Keane JR, Segall HD, Zee CS. **CT observations pertinent to septic cavernous sinus thrombosis.** *AJNR Am J Neuroradiol* 1985;6:755-758
7. Yarrington CT. **Cavernous sinus thrombosis revisited.** *Proc R Soc Med* 1977;70:456-459
8. Levine ST, Twyman RE, Gilman S. **The role of anticoagulation in cavernous sinus thrombosis.** *Neurology* 1988;38:17-522
9. Schuknecht B, Simmen D, Wichmann W, Valavanis A. **MR identification of carotid artery involvement in septic cavernous sinus thrombosis.** *Int J Neuroradiol* 1996;290-295
10. Berge J, Louail C, Caille JM. **Thrombophlébite du sinus caverneux stratégie diagnostique.** *J Neuroradiol* 1994;21:191-117
11. Kriss TC, Kriss VM, Warf BC. **Cavernous sinus thrombophlebitis: case report.** *Neurosurgery* 1996;39:385-389
12. Lillie HI. **Prognosis of septic thrombophlebitis of the cavernous sinus.** *J Int Coll Surg* 1951;15:754-759
13. Palmershein LA, Hamilton MK. **Fatal cavernous sinus thrombosis secondary to third molar removal.** *Am Assoc Oral Maxillofac Surg* 1982;40:371-376
14. Hosoya T, Kera M, Suzuki T, Yamaguchi K. **Fat in the normal cavernous sinus.** *Neuroradiology* 1986;28:264-266
15. Daniels DL, Czervionke LF, Bonneville JF, et al. **MR imaging of the cavernous sinus: value of spin echo and gradient recalled echo images.** *AJNR Am J Neuroradiol* 1988;9:947-952
16. Hirsch WL Jr, Hryshko FG, Sekhar LN, et al. **Comparison of MR imaging, CT, and angiography in the evaluation of the enlarged cavernous sinus.** *AJNR Am J Neuroradiol* 1988;9:907-915
17. Yarrington CT. **The prognosis and treatment of cavernous sinus thrombosis.** *Ann Rhinol Laryngol Otol* 1961;70:263-267
18. Karlin RJ, Robinson WA. **Septic cavernous sinus thrombosis.** *Ann Emerg Med* 1984;13:449-455
19. Tvetras K, Kristensen S, Dommerby H. **Septic cavernous and lateral sinus thrombosis.** *J Laryngol Otol* 1988;102:877-882
20. Ellie E, Houang B, Louail C, et al. **CT and high-field MRI in septic thrombosis of the cavernous sinuses.** *Neuroradiology* 1992;34:22-24
21. Macdonald RL, Findlay JM, Tator CH. **Sphenothmoidal sinusitis complicated by cavernous sinus thrombosis and pontocerebellar infarction.** *Can J Neurol Sci* 1988;15:310-313
22. Dyken ME, Biller J, Fincham R, Moore SA. **Carotid-cavernous sinus thrombosis caused by aspergillus fumigatus: magnetic resonance imaging with pathologic correlation.** *Angiology* 1990;652-657
23. Sekhar LN, Dujovny M, Rao GR. **Carotid-cavernous sinus thrombosis caused by aspergillus fumigatus.** *J Neurosurg* 1980;52:120-125
24. Ben-Uri R, Palma L, Kaveh Z. **Case report: septic thrombosis of the cavernous sinus: diagnosis with the aid of computed tomography.** *Clin Radiol* 1989;40:520-522
25. Endo S, Ohtsui T, Fukuda O, Oka N, Takaku A. **A case of septic cavernous sinus thrombosis with sequential dynamic angiographic changes.** *Surg Neurol* 1989;32:59-63
26. Gupta A, Jalali S, Bansal RK, Grewal SPS. **Anterior ischemic optic neuropathy and branch retinal artery occlusion in cavernous sinus thrombosis.** *J Clin Neuroophthalmol* 1990;10:193-196
27. Assefa D, Dalitz E, Handrick W, Lietz R, Braun W, Michalski H. **Septic cavernous sinus thrombosis following infection of ethmoidal and maxillary sinuses: a case report.** *Int J Pediatr Otorhinolaryngol* 1994;29:249-255
28. Chung JW, Chang KH, Han MH, Kim BH, Song CS. **Computed tomography of cavernous sinus diseases.** *Neuroradiology* 1988;30:319-328
29. Saah D, Schwartz A. **Diagnosis of cavernous sinus thrombosis by magnetic resonance imaging using flow parameters.** *Ann Otol Rhinol Laryngol* 1994;103:487-489
30. Doyle KJ, Jackler RK. **Otogenic cavernous sinus thrombosis.** *Otolaryngol Head Neck Surg* 1991;104:873-877
31. Kline LB, Acker JD, Donovan Post MJ, Vitek JJ. **The cavernous sinus: a computed tomographic study.** *AJNR Am J Neuroradiol*

- 1981;2:299-305
32. Kline LB, Acker JD, Donovan Post MJ. **Computed tomographic evaluation of the cavernous sinus.** *Ophthalmology* 1982;89:374-385
33. Hasso AN, Pop PM, Thompson JR, et al. **High resolution thin section computed tomography of the cavernous sinus.** *Radiographics* 1982;2:83-100
34. Korogi Y, Takahashi M, Sakamoto Y, Shinzato J. **Cavernous sinus: correlation between anatomic and dynamic gadolinium-enhanced MR imaging findings.** *Radiology* 1991;180:235-237
35. Stricof DD, Gabrielsen TO, Latack JT, Gebarski SS, Chandler WF. **CT demonstration of cavernous sinus fat.** *AJNR Am J Neuroradiol* 1989;10:1199-1201
36. Mahapatra AK. **Brain abscess: an unusual complication of cavernous sinus thrombosis.** *Clin Neurol Neurosurg* 1988;90:241-243